MODEL ORDER REDUCTION OF NON-LINEAR MAGNETOSTATIC PROBLEMS BASED ON POD AND DEI METHODS

T. Henneron[1] and S. Clénet[2]

[1]L2EP/Université Lille1, Cité Scientifique - 59655 Villeneuve d'Ascq, France
[2] L2EP/Arts et Métiers ParisTech, Centre de Lille, 8 boulevard Louis XIV - 59046 Lille Cedex, France

In the domain of numerical computation, Model Order Reduction approaches are more and more frequently applied in mechanics and have shown their efficiency in terms of reduction of computation time and memory storage requirements. One of these approaches, the Proper Orthogonal Decomposition (POD), can be very efficient in solving linear problems but encounters limitations in the non-linear case. In this paper, the Discret Empirical Interpolation Method coupled with the POD method is presented. This is an interesting alternative to reduce large-scale systems deriving from the discretization of non-linear magnetostatic problems coupled with an external electrical circuit.

***Index Terms*— Discret Empirical Interpolation Method, Model Order Reduction, Non-linear Problem, Proper Orthogonal Decomposition, Static fields.**

I. INTRODUCTION

TO DESCRIBE the behavior of electrical machines coupled with an external electrical circuit, the Finite Element Method associated with a time-stepping scheme is often used to numerically solve Maxwell's equations coupled with the circuit equations. When a fine mesh and a small time step are used, the computation time of the large-scale system obtained from the discretization of the Non-Linear Partial Differential Equations (NL-PDE) can be prohibitive. To tackle this issue, an alternative method is to apply model order reduction methods. In the literature, the Proper Orthogonal Decomposition has been widely used to solve many problems in engineering [1]. This method consists of performing a projection onto a reduced basis, meaning the size of the equation system to solve can be highly reduced. The snapshot approach is the most popular to determine the discrete projection operator between the original basis (generating from the mesh) and the reduced basis [2]. In computational electromagnetics, the POD method has been applied to study the behavior of a transformer with a non-linear core [3][4] or to solve magnetoquasistatic and electroquasistatic field problems [5][6]. In the case of linear PDEs, the POD approach can lead to a dramatic reduction in the computation time. In the non-linear case, this method is not quite as efficient due to the computation cost of the non-linear terms in the reduced system, which requires the assembling of the equation system of the full initial problem. To tackle this issue, the Discret Empirical Interpolation Method (DEIM) method can be coupled with the POD approach [7]. DEIM interpolates the non-linear behavior of the magnetic field on the whole spatial domain from evaluations of the non-linear behavior law on a reduced number of localized regions. The determination of such localized regions is automatic and does not require any intervention from the user. The computation time of the non-linear terms when applying the POD is thus highly reduced.

In this paper, the DEIM-POD approach is applied to solve a non-linear magnetostatic problem coupled with an electrical circuit using the vector potential formulation. First, the numerical model is presented. Secondly, the Snapshot POD method and the DEIM are developed. Finally, non-linear models based solely on either the POD method or the DEIM-POD are compared. The results obtained with the reduced models are also compared in terms of accuracy and computation time using the full Finite Element model.

Manuscript received January 1, 2008 (date on which paper was submitted for review). Corresponding author: T. Henneron (e-mail: Thomas.henneron@univ-lille1.fr).
Digital Object Identifier inserted by IEEE

II. NON-LINEAR MAGNETOSTATIC PROBLEM COUPLED WITH ELECTRIC CIRCUIT

Let us consider a domain D of boundary Γ ($\Gamma=\Gamma_B\cup\Gamma_H$ and $\Gamma_B\cap\Gamma_H=0$) (Fig. 1). The problem is solved on D×[0,T] with T the width of the time interval. The source field is created by a stranded inductor supplied by a voltage v(t).

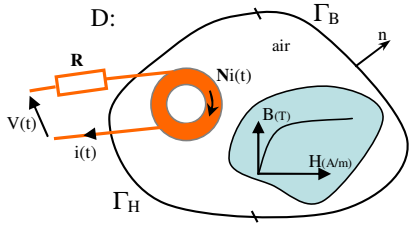

Figure 1. Non-linear magnetostatic problem coupled with electrical circuit

In magnetostatics, the problem can be described by the following equations:

$$\mathbf{curl}\ \mathbf{H}(\mathbf{x},t) = \mathbf{N}(\mathbf{x})i(t) \quad (1)$$

$$\mathrm{div}\ \mathbf{B}(\mathbf{x},t) = 0 \quad (2)$$

$$\mathbf{H}(\mathbf{x},t) = \nu_{(\mathbf{B})}(\mathbf{x})\,\mathbf{B}(\mathbf{x},t) \quad (3)$$

with **B** the magnetic flux density, **H** the magnetic field, **N** and i the unit current density and the current flowing through the stranded inductor and finally $\nu_{(\mathbf{B})}(\mathbf{x})$ the reluctivity. For the ferromagnetic material, $\nu_{(\mathbf{B})}(\mathbf{x})$ may depend on **B** in the non-linear case. To impose the uniqueness of the solution, boundary conditions must be added such that:

$$\mathbf{B}(\mathbf{x},t).\mathbf{n}=0 \text{ on } \Gamma_B \text{ and } \mathbf{H}(\mathbf{x},t)\times\mathbf{n}=0 \text{ on } \Gamma_H \quad (4)$$

with **n** the outward unit normal vector. In order to impose the voltage v(t) at the terminals of the stranded inductor, the following relation must be considered:

$$\frac{d\Phi(t)}{dt} + Ri(t) = v(t) \tag{5}$$

with R the resistance of the inductor and Φ the flux linkage.

The previous problem can be solved by introducing the vector potential **A**. From (2)**,** this potential is defined such that $\mathbf{B}(\mathbf{x},t)=\mathbf{curlA}(\mathbf{x},t)$ with $\mathbf{A}(\mathbf{x},t)\times\mathbf{n}=0$ on Γ_B. To take into account the non-linear behavior of the ferromagnetic material, the fixed point technique can be used [8]. In this case, the magnetic field $\mathbf{H}(\mathbf{x},t)$ can be expressed by $\mathbf{H}(\mathbf{x},t)=\nu_{fp}\mathbf{B}(\mathbf{x},t)+\mathbf{H}_{fp}(\mathbf{B}(\mathbf{x},t))$ with ν_{fp} a constant and $\mathbf{H}_{fp}(\mathbf{B}(\mathbf{x},t))=(\nu_{(\mathbf{B})}(\mathbf{x})-\nu_{fp})\mathbf{B}(\mathbf{x},t)$ a virtual magnetization vector. According to (1) and (5), the equations to solve are

$$\mathbf{curl}(\nu_{fp}\mathbf{curlA}(\mathbf{x},t)) - \mathbf{N}(\mathbf{x})i(t) = -\mathbf{curl}(\mathbf{H}_{fp}(\mathbf{curlA}(\mathbf{x},t))), \tag{6}$$

$$\frac{d}{dt}\int_D \mathbf{A}(\mathbf{x},t).\mathbf{N}(\mathbf{x})dD + Ri(t) = v(t). \tag{7}$$

To ensure the unicity of the solution, a gauge condition must be added. To solve this problem, $\mathbf{A}(\mathbf{x},t)$ and $\mathbf{N}(\mathbf{x})$ are discretised using edge and facet elements [9]. We denote $A_i(t)$ the value of **A** along the i^{th} edge and N_e the number of edges. Then, applying the Galerkin method to (6) and (7), a system of differential algebraic equations is obtained

$$\mathbf{MX}(t) + \mathbf{K}\frac{d\mathbf{X}(t)}{dt} = \mathbf{F}(t) - \mathbf{M}_{fp}(\mathbf{X}(t)) \tag{8}$$

with $\mathbf{X}(t)$ the vector of unknowns of size $N_{un}=N_e+1$ such that $(X_i(t))_{1\le i\le Ne} = (A_i(t))_{1\le i\le Ne}$ and $X_{Nun}(t) = i(t)$. **M** and **K** are $N_{un}\times N_{un}$ matrices and $\mathbf{F}(t)$ and $\mathbf{M}_{fp}(\mathbf{X}(t))$ $N_{un}\times 1$ vectors.

III. Model Order Reduction With DEIM-POD

A. Proper Orthogonal Decomposition

In order to reduce the computation time required to solve system (8), the POD method is applied [1]. The vector $\mathbf{X}(t)$ is approximated in a reduced basis by a vector $\mathbf{X}_r(t)$ of size N_s ($N_s<<N_{um}$). To obtain a discrete projection operator $\mathbf{\Psi}$ such that

$$\mathbf{X}(t) = \mathbf{\Psi}\mathbf{X}_r(t), \tag{9}$$

the snapshot approach is typically applied [2]. The system (8) is solved for the first N_s time steps (called snapshots). The snapshot matrix $\mathbf{M}_s$ is defined by $\mathbf{M}_s=(\mathbf{X}^j)_{1\le j\le Ns}$ with $\mathbf{X}^j$ the solution $\mathbf{X}(t)$ at the j^{th} time step. Applying the Singular Value Decomposition (SVD), $\mathbf{M}_s$ can be decomposed under the form:

$$\mathbf{M}_s=\mathbf{V\Sigma W}^t \tag{10}$$

with $\mathbf{V}_{Nun\times Nun}$ and $\mathbf{W}_{Ns\times Ns}$ orthogonal matrices and $\mathbf{\Sigma}_{Nun\times Ns}$ the diagonal matrix of the singular values. The i^{th} row of **W** represents the entries of the i^{th} vector of the matrix $\mathbf{M}_s$ projected in the reduced basis formed by the N_s vectors of the matrix $\mathbf{V\Sigma}$. The operator $\mathbf{\Psi}$ is then given by normalizing the matrix $\mathbf{V\Sigma}$ or $\mathbf{M}_s\mathbf{W}$. Finally, in the reduced basis, the new system to solve can be deduced combining (8) and (9)

$$\mathbf{M}_r\mathbf{X}_r(t) + \mathbf{K}_r\frac{d\mathbf{X}_r(t)}{dt} = \mathbf{\psi}^t\mathbf{F}(t) - \mathbf{\psi}^t\mathbf{M}_{fp}(\mathbf{\Psi}\mathbf{X}_r(t)) \tag{11}$$

$$\text{with } \mathbf{M}_r = \mathbf{\Psi}^t\mathbf{M}\mathbf{\Psi} \text{ and } \mathbf{K}_r = \mathbf{\Psi}^t\mathbf{K}\mathbf{\Psi}.$$

In practical terms, the computational time of the SVD of $\mathbf{M}_s$ can be prohibitive due to its size which depends on N_{un} and N_s. To tackle this issue, the matrix of correlations $\mathbf{C}_s$ of $\mathbf{M}_s$ is used. This matrix is determined such that

$$\mathbf{C}_s = \frac{1}{N_s}\mathbf{M}_s^t\mathbf{M}_s \tag{12}$$

The size of $\mathbf{C}_s$ is $N_s\times N_s$. The eigenvalue decomposition of $\mathbf{C}_s$ can be applied to obtain the matrix **W** because $\mathbf{C}_s = \mathbf{W\Sigma V}^t\ \mathbf{V\Sigma W}^t = \mathbf{W\Delta W}^t$. In this case, the complexity and the computational time to determine **W** is highly reduced compared to a SVD of $\mathbf{M}_s$.

B. Discret Empirical Interpolation Model with POD

In the non-linear case, the computational complexity of the vector $\mathbf{f}_{nl}(t) = \mathbf{M}_{fp}(\mathbf{\Psi}\mathbf{X}_r(t))$ can be significant (see (12)). In fact, it is necessary to evaluate the solution $\mathbf{X}(t)=\mathbf{\Psi}\mathbf{X}_r(t)$ in the original basis to determine the vector $\mathbf{M}_{fp}(\mathbf{X}(t))$. To tackle this issue, an alternative is to apply the DEIM [7]. This approach proposes to approximate the non-linear function $\mathbf{f}_{nl}(t)$ by combining projections with interpolations. All the entries of the vector $\mathbf{f}_{nl}(t)$ no longer need to be evaluated. The approximation of $\mathbf{f}_{nl}(t)$ is determined from a linear combination of a limited number entries of $\mathbf{f}_{nl}(t)$ selected automatically applying the DEIM. The j^{th} entry $f_{nl}^j(t)$ of the vector $\mathbf{f}_{nl}(t)$ is equal to the integral over the domain of $\mathbf{curl}\,\mathbf{H}_{fp}$ weighted by the edge shape function $\mathbf{w}_j$. Since $\mathbf{w}_j$ is null except on the elements connected to the j^{th} edge denoted by supp{j}, the calculation of $f_{nl}^j(t)$ is local just requiring the circulations of **A** along the edges belonging to the j^{th} edge to be able to evaluate $\mathbf{H}_{fp}$ everywhere on supp{j}. For this reason, the calculation of this selected terms of $\mathbf{f}_{nl}(t)$ is then very fast. We seek to approximate $\mathbf{f}_{nl}(t)$ by

$$\mathbf{f}_{nl}(t) = \mathbf{U}\mathbf{c}(\mathbf{X}_r(t)) \tag{13}$$

with $\mathbf{c}(\mathbf{X}_r(t))$ the interpolation vector of size $N_{deim}\times 1$ and **U** an orthogonal $N_{um}\times N_{deim}$ matrix calculated by applying a POD method with the vectors $\mathbf{M}_{fp}(\mathbf{X}(t))$ on the N_{deim} first time steps. The system (13) is over-determined. To express the coefficients of $\mathbf{c}(\mathbf{X}_r(t))$, N_{deim} distinct rows from the over-determined system are selected by applying a matrix **P** such as $\mathbf{P}^t\mathbf{f}_{nl}(t)= \mathbf{P}^t\mathbf{U}\mathbf{c}(\mathbf{X}_r(t))$. The algorithm presented in [7] is used to determine the matrix $\mathbf{P}=(\mathbf{I}_i)_{1\le i\le Ndeim}$ with $\mathbf{I}_i$ a column of the identity matrix $\mathbf{I}_{Nun\times Nun}$. The DEIM algorithm thus extracts a set of indices which correspond to the DEIM edges. Then, $\mathbf{c}(t)$ can be expressed by

$$\mathbf{c}(t)=(\mathbf{P}^t\mathbf{U})^{-1}\,\mathbf{P}^t\mathbf{f}_{nl}(t) = (\mathbf{P}^t\mathbf{U})^{-1}\,\mathbf{P}^t\mathbf{M}_{fp}(\mathbf{\Psi}\mathbf{X}_r(t)) \tag{14}$$

Moreover, in the case of a non-linear magnetostatic problem coupled with an electrical circuit, it can be shown that, in (14), the vector $\mathbf{P}^t\mathbf{M}_{fp}(\mathbf{\Psi X}_r(t))$ is equivalent to $\mathbf{M}_{fp}(\mathbf{P}^t\mathbf{\Psi X}_r(t))$. Finally, by combining (13) and (14), the vector $\mathbf{f}_{nl}(t)$ is approximated by

$$\mathbf{f}_{nl}(t) = \mathbf{M}_{fp}(\mathbf{X}(t)) \approx \mathbf{U}(\mathbf{P}^t\mathbf{U})^{-1}\mathbf{M}_{fp}(\mathbf{P}^t\mathbf{\Psi}^t\mathbf{X}_r(t)) \qquad (15)$$

In this expression, the calculation of the term $\mathbf{M}_{fp}(\mathbf{P}^t\mathbf{\Psi X}_r(t))$ simply requires the evaluation at the N_{deim} DEIM edges of the non-linear function, and not at all edges, as in (11), to interpolate the term $\mathbf{M}_{fp}(\mathbf{X}(t))$. In practical terms, the term $\mathbf{\Psi}^t\mathbf{U}(\mathbf{P}^t\mathbf{U})^{-1}$ is only calculated once.

IV. Application

A 3D magnetostatic example, made of a single phase EI transformer at no load supplied at 50Hz with a sinusoidal voltage, is studied. Due to the symmetry, only one eighth of the transformer is modeled (Fig. 2). The non-linear magnetic behavior of the iron core is considered. The 3D spatial mesh is made of 12659 nodes and 67177 tetrahedrons. The Euler scheme is used to solve (11) with 30 time steps per period.

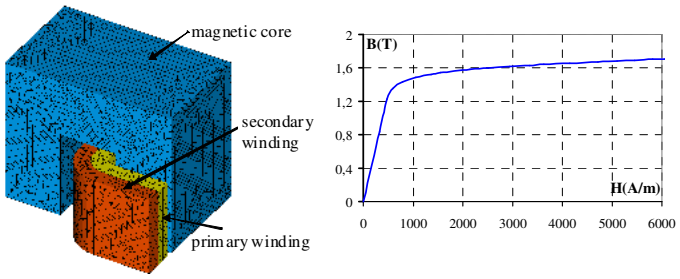

Figure 2. Example of application (a: geometry, b: non-linear curve of the core)

In the following, we compare the results obtained from the POD and DEIM-POD reduced models with those obtained using the full model. The solution given by the full model will be considered as the reference.

A. *Influence of the number of snapshots on the evolution of the current*

In order to evaluate the influence of the number of snapshots on a global value, the evolutions of the current i(t) versus time, obtained from the POD and DEIM-POD models, are compared with the reference in Fig. 3 and Fig. 4. The N_s snapshots correspond to the vector $\mathbf{A}$ for the N_s first time steps of the full model. The size of the reduced model (11) is equal to the number of snapshots. The reduced model is then run again starting at t=0. The number of snapshots influences the evolution of the current for both reduced models. The POD models as expected gives the same results as the full model for the N_s first time step and then it appears a divergence. This property is not satisfies anymore with the DEIM-POD method since the non-linearity is not accounted as in the full model. We can observe that the current waveform converges towards the reference with both approaches when N_s increases. In order to estimate the convergence versus the number of snapshots, an error estimator ε_i is defined

$$\varepsilon_i = \frac{\|\mathbf{i}_{ref} - \mathbf{i}_{red}\|_2}{\|\mathbf{i}_{ref}\|_2} \qquad (16)$$

with $\mathbf{i}_{ref}$ and $\mathbf{i}_{red}$ the vectors of current values at each time step obtained from the reference and the POD (or DEIM-POD) model respectively. Figure 5 presents the evolution of ε_i versus the number of snapshots. We can see that the convergence is faster with POD where the non-linear vector $\mathbf{M}_{fp}$ in (11) is evaluated for all edges of the mesh. In the case of the DEIM-POD model, this vector is interpolated with a low number of edges using (15). In our case, the number of DEIM edges is equal to the number of snapshots. Then, the number of DEIM edges must be sufficient to obtain a good interpolation of the vector $\mathbf{M}_{fp}(\mathbf{\Psi X}_r(t))$. This vector is correctly expressed with 8 DEIM edges. The error on the current is equal to 0.03%. For the same number of snapshots, the error is 0.004% for the POD model. The DEIM-POD approach requires more snapshots to obtain a result very close to that of the reference than the POD model. Figure 6 presents the edges selected automatically by the DEIM for 8 snapshots. As expected, these edges are located in the saturated area.

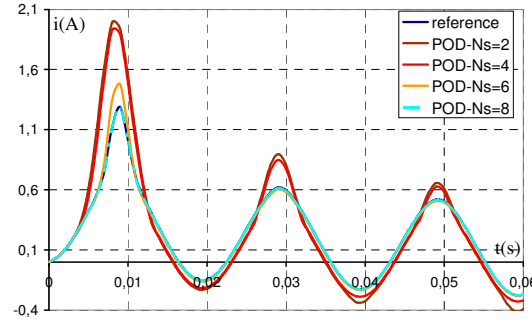

Figure 3. Evolution of the current obtained from the POD model

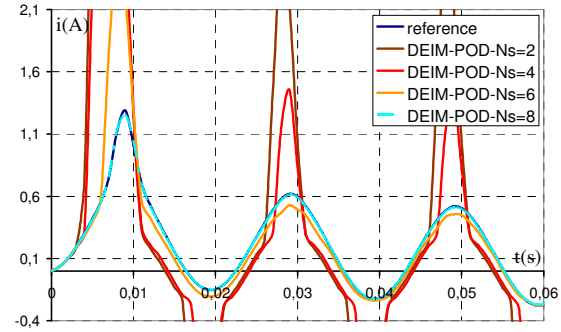

Figure 4. Evolution of the current obtained from the DEIM-POD model

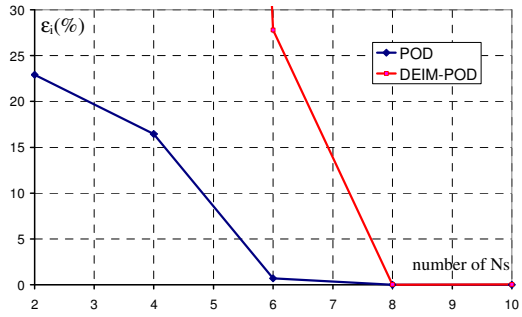

Figure 5. Error of the current versus the number of snapshots

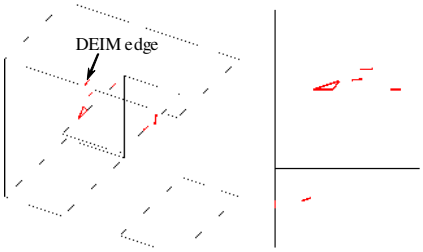

Figure 6. DEIM edges in the magnetic core (a: 3D view, b: view of top)

B. *Influence of the number of snapshots on the distribution of the fields*

According to (9), the vector solution is approximated by a linear combination of vector $\mathbf{\Psi}_j$ of $\mathbf{\Psi}$, often called a mode. Each $\mathbf{\Psi}_j$ corresponds to a field distribution. Figures 7 and 8 present the field distribution corresponding to $\mathbf{\Psi}_j$ for the first four modes in the magnetic core. The distribution corresponding to $\mathbf{\Psi}_1$ and $\mathbf{\Psi}_2$ are close to a physical distribution of the magnetic flux density encountered in a transformer. The distributions corresponding to $\mathbf{\Psi}_3$ and $\mathbf{\Psi}_4$ have no physical meaning except that they enable us to better take into account the saturation at the corner of the core.

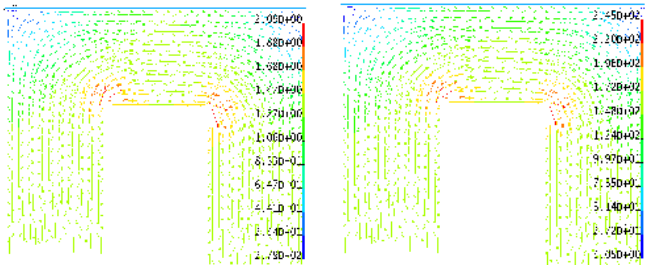

Figure 7. Distributions of $\mathbf{\Psi}_1$ (a) and $\mathbf{\Psi}_2$ (b)

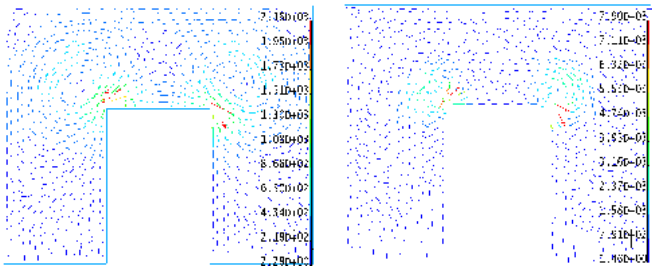

Figure 8. Distributions of $\mathbf{\Psi}_3$ (a) and $\mathbf{\Psi}_4$ (b)

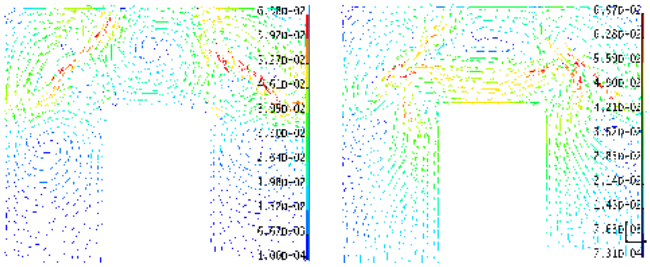

Figure 9. Distribution of the difference between the magnetic flux density obtained by the reference model and the POD (a) and DEIM-POD (b) (t=10ms)

In figure 9, the error of the distribution determined with the POD and DEIM-POD models for 8 snapshots are given. Their distributions express the truncation of the solution between the reference model and the reduced models. If we increase the number of snapshots, the error will decrease. We can observe that the distributions of the error are different between the POD and DEIM-POD models. This difference can be explained by the interpolation of the non-linear term in the case of the DEIM-POD model.

C. *Computation time*

In terms of computation time, with a time interval width of 0.12s and 120 time steps, the reference model requires 130min. For 8 snapshots, the computation time is 24min with the POD and 11min with the DEIM-POD. These computation times do not take into account the computation time required to evaluate the solutions of the snapshots: for 8 snapshots, the computation time is 8min42s. The DEIM-POD model is faster than the POD model, the ratio being 2.2. This ratio is a function of the number of elements in the magnetic core. With a finer mesh and a fixed number of snapshots, the computation time required to evaluate the non-linear term $\mathbf{M}_{fp}(\mathbf{\Psi X}_r(t))$ in (11) is more significant and thus, the computation time ratio for the non-linear term between the POD and DEIM-POD models increases.

V. Conclusion

The Proper Orthogonal Decomposition and the Discret Empirical Interpolation Method associated with a FEM vector potential formulation have been developed in order to solve a 3D non-linear magnetostatic problem coupled with an external circuit. Based on the example here, it has been shown that the POD model associated with the DEIM enables us to reduce the computation time significantly while obtaining good precision. In this paper, the fixed point technique has been used to account for the non linearity. Future work will be to extend the application of the POD-DEIM when the Newton Raphson method is applied.

References

[1] J. Lumley, "The structure of inhomogeneous turbulence", *Atmospheric Turbulence and Wave Propagation*. A.M. Yaglom and V.I. Tatarski., pp. 221–227, 1967.

[2] L. Sirovich, "Turbulence and the dynamics of coherent structures", *Q. Appl. Math.*, vol. XLV, no. 3, pp. 561–590, 1987.

[3] Y. Zhai, "Analysis of Power Magnetic Components With Nonlinear Static Hysteresis: Proper Orthogonal Decomposition and Model Reduction", *IEEE Trans. Magn.*, vol. 43(5), pp. 1888-1897, 2007.

[4] T. Henneron, S. Clénet, "Model Order Reduction of Electromagnetic Field Problem Coupled with Electric Circuit Based on Proper Orthogonal Decomposition", *Proceeding of OIPE* (Ghent), 2012.

[5] D. Schmidthäusler, M. Clemens, "Low-Order Electroquasistatic Field Simulations Based on Proper Orthogonal Decomposition", *IEEE Trans. Magn.*, vol. 48(2), pp. 567-570, 2012.

[6] T. Henneron, S. Clénet, "Model order reduction of quasi-static problems based on POD and PGD approaches", *EPJ AP*, to be published.

[7] S. Chaturantabut and D. C. Sorensen, "Nonlinear Model Reduction via Discrete Empirical Interpolation*", SIAM J. Sci. Comput.*, vol. 32(5), pp.2737–2764, 2010.

[8] M. Chiampi, D. Chiarabaglio, M. Repetto, "A jiles-Atherton and Fixed-point Combined Technique for Time Periodic Magnetic field Problems with Hysteresis", *IEEE Trans. Magn.*.vol. 31(6), pp 4306-4311, 1995.

[9] A. Bossavit, "A rationale for edge-elements in 3-D fields computations", *IEEE Trans. Magn.*.vol. 24(1), pp 74-79, 1988.